# Chapter 1

Post-Denitration Reactions

1.1 Introduction

Products of the preliminary denitration step of **NC!** (**NC!**) can be evolved as gases or remain trapped in the polymer matrix. Reactive nitrogen dioxide radicals generated from homolysis of the O-N bond are likely to migrate within the bulk and attack other sites on the polysaccharide, initiating branched radical chain reactions. These lead to deeper decomposition of the polymer *via* chain scission and rupture of glucose rings, with eventual complete disintegration of the molecule, assisted by products released by ongoing acid hydrolysis. Nitrous and nitric acids are released directly from denitration or via transformation of released NO_x species. In addition to catalysing hydrolysis, they increase the acidity of the overall system, lowering the pH and stimulating further hydrolytic processes [1]. The final product mixture is dictated by the numerous side reactions involving autocatalysis, radical reactions and product interactions.

When studying the ageing of **NC!** using **UVVis!** spectroscopy, Moniruzzaman *et al.* observed increasing concentrations of reaction products beyond those generated from first-stage decomposition, following heat treatment over extended timescales [2, 3]. The reaction of the **SB59!** (**SB59!**) with NO_x released by denitration, mimics the action of stabilisers such as **DPA!** (**DPA!**) and **2NDPA!** (**2NDPA!**) commonly used in **NC!** formulations. The secondary amine groups of the dye consume any nitrates in the system, eliminating the possibility of successive reactions generating acidic species. Un-aged **NC!** thin films, and films aged at 40°C, 50°C, 60°C and 70°C for timescales of up to 2000hrs for 40°C, were compared. **UV!** absorbances at 600 nm and 650 nm were characteristic of the **SB59!** dye used to indicate the presence of NO_x, released by the denitration of **NC!** (figure 1.2). The isosbestic point identified at 552 nm showed a proportional relationship between the
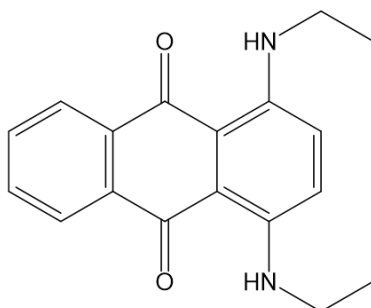
Figure 1.1: SB59! (**SB59!**) used to probe the release of nitrates from **NC!** using **UVVis!** (**UVVis!**) and ^{1}H NMR spectroscopy [3]. The action of nitrate absorption by the dye imitates that of stabilisers commonly used with nitrate ester formulations.

(a) NC! film aged at 40°C.

(b) NC! film aged at 50°C.

(d) NC! film aged at 70°C.

(c) NC! film aged at 60°C.
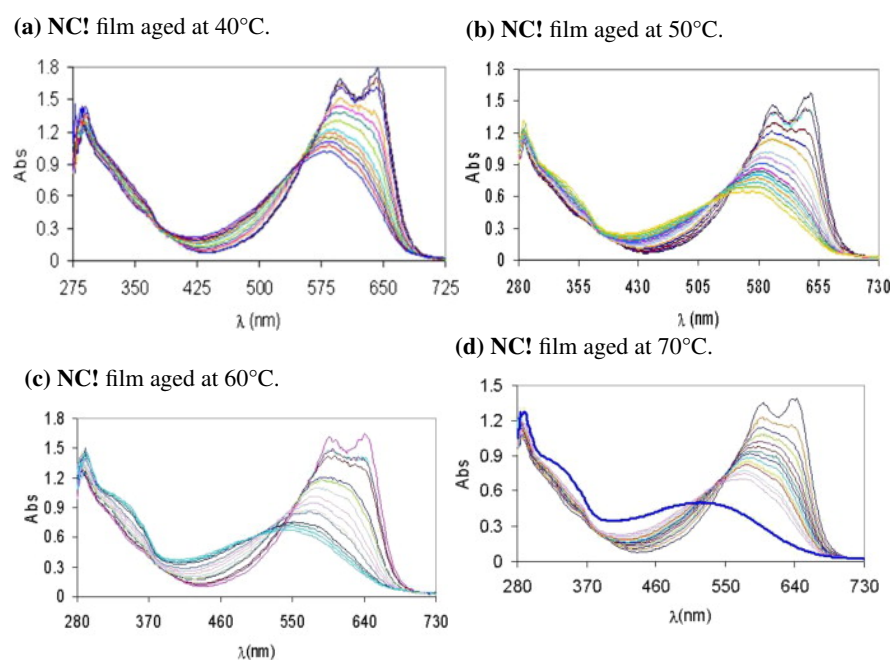
Figure 1.2: UVVis! spectra of aged **NC!**-based film, from the work of Moniruzzaman *et al.*[3]. The peaks at 600 nm and 650 nm are attributed to the π - π^* transitions in the anthraquinone dye (**SB59!**). Spectral lines with highest absorbance peaks in this region correspond to the sample prior to heat treatment. Peaks below 400 nm indicate the formation of **SB59!** derivatives due to secondary reactions.
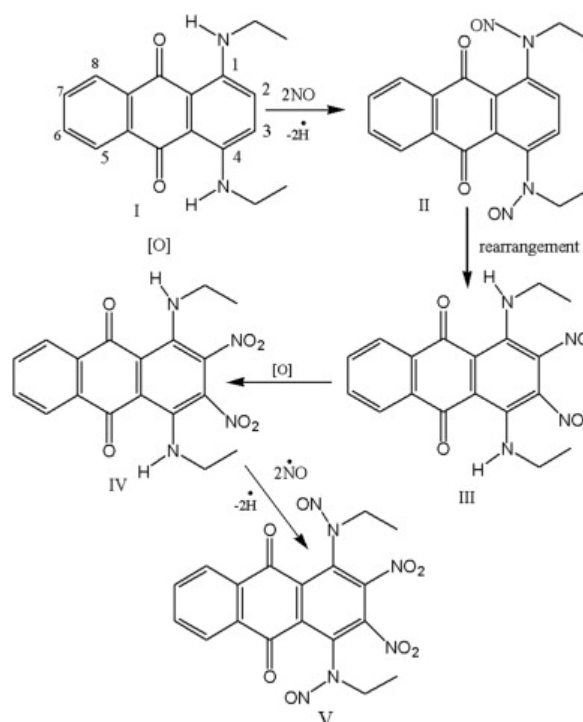
Figure 1.3: Proposed pathway for the reaction of **SB59!** dye with ˙NO released as a result of deni-
tration of **NC!** [3].

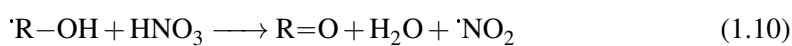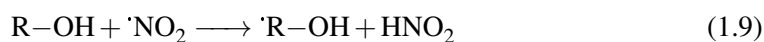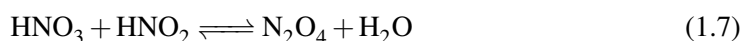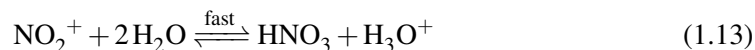concentration of **SB59!** as it decreased, with the concentration of the [**SB59! + NC!**] product
as it increased. Samples exposed to higher ageing temperatures presented spectra dominated
by products formed *via* secondary reactions. For samples aged at temperatures >40°C, the
isosbestic point demonstrated a downwards shift with increasing dye consumption. In the
case of the 70°C treated run, the final measurement (indicated by the royal-blue line in bold
in figure 1.2d)) deviated from the isosbestic point entirely, with more than 81% consumption
of the original dye concentration. The drift from the isosbestic point, in addition to the
appearance of new absorbance peaks below 400 nm, allude to the presence of new species
in the reaction mixture not generated by the primary reaction of **SB59!** and **NC!**. It is likely
that these arise from the continued reaction of **SB59!** derivatives with **NC!** degradation
products, or further derivatives thereof, as suggested in figure 1.3. Following cleavage
of the nitrate ester via homolytic fission, elimination of nitrous acid, or hydrolysis, the
resulting residues available for further reaction with the polymer or other free molecules in
the system. In the study of **PETN!** (**PETN!**) ageing at high temperatures (115 °C - 135 °C)
in vacuum, and low temperatures (20 °C - 65 °C) in acetonitrile solution, Shepodd *et al.*
commented that thermolysis produced a more complex and varied mixture, due to deeper
degradation and recombination of radicals [**?**]. By contrast, the low temperature hydrolytic

Thermolytic initiation

$$R-ONO_2 \longrightarrow R-O^{\cdot} + {}^{\cdot}NO_2 \tag{1.1}$$

Propagation

$$R-O^{\cdot} + {}^{\cdot}NO_2 \xrightarrow{R-ONO_2} R-ONO_2 + {}^{\cdot}NO + {}^{\cdot}NO_2 + N_2O_4$$
$$+ H_2O + N_2O + CO_2 + CO$$
$$+ C_2H_2O + \text{other organic fragments} \tag{1.2}$$

$$2\,{}^{\cdot}NO + O_2 \longrightarrow 2\,{}^{\cdot}NO_2 \tag{1.3}$$

$$2\,{}^{\cdot}NO_2 \rightleftharpoons N_2O_4 \tag{1.4}$$

Hydrolytic initiation

$$R-ONO_2 + H_2O \longrightarrow R-OH + HNO_3 \tag{1.5}$$

$$R-OH + HNO_3 \longrightarrow R{=}O + HNO_2 + H_2O \tag{1.6}$$

Propagation

$$HNO_3 + HNO_2 \rightleftharpoons N_2O_4 + H_2O \tag{1.7}$$

$$N_2O_4 \rightleftharpoons 2\,{}^{\cdot}NO_2 \tag{1.8}$$

$$R-OH + {}^{\cdot}NO_2 \longrightarrow {}^{\cdot}R-OH + HNO_2 \tag{1.9}$$

$${}^{\cdot}R-OH + HNO_3 \longrightarrow R{=}O + H_2O + {}^{\cdot}NO_2 \tag{1.10}$$
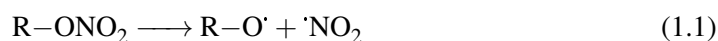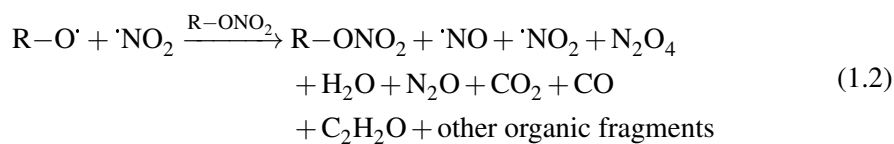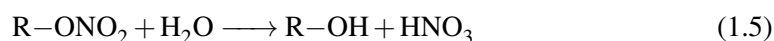
process emphasised formation of **PETRIN!** (**PETRIN!**) followed by side reactions with reduced likelihood of radical recombination in solution compared to in a solid , as ${}^{\cdot}NO_2$ would be more likely to diffuse and react elsewhere. Chin *et al.* proposed schemes for the propagation of secondary reactions initated by both the thermolysis (scheme **??**) and hydrolysis of nitrate esters (scheme **??**) [4].

Termination reactions were not emphasised in either of the schemes for these cases. The hydrolysis scheme was adapted from an earlier work by Camera *et al.* (first referenced in section **??**) involving the nitrate ester decomposition and subsequent reactions of ethyl nitrate (where R = CH_3CH_2 for the scheme above) [5]. The original study included an expansion of the hydrolysis step (equation equ:protonation,), where the involvement of $NO_2{}^{+}$ was illustrated (scheme **??**

It was highlighted by Camera, that the oxidation of alcohol by nitric acid (equation 1.6) is slow and thus rate-limiting. The mechanism is likely to occur *via* a series of intermediate

Hydrolysis scheme for ethyl nitrate

$$CH_3CH_2ONO_2 + H^+ \stackrel{fast}{\rightleftharpoons} CH_3CH_2ONO_2H^+ \tag{1.11}$$

$$CH_3CH_2ONO_2H^+ \stackrel{slow}{\rightleftharpoons} CH_3CH_2OH + NO_2^+ \tag{1.12}$$

$$NO_2^+ + 2\,H_2O \stackrel{fast}{\rightleftharpoons} HNO_3 + H_3O^+ \tag{1.13}$$
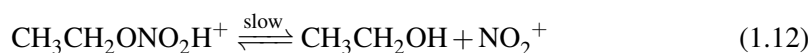
reactions of which the details are not known. Following the generation of nitrous acid, subsequent oxidations occur rapidly. According to Rigas *et al.*, alcohols are more susceptible to wet oxidation than esters [6]. A higher concentration of unsubstituted hydroxyl groups in the system, and therefore a fewer nitrate ester groups (or a lower **DOS!** (**DOS!**) value), decreases overall stabililty.
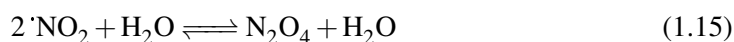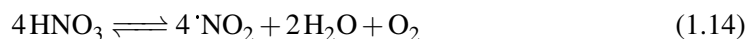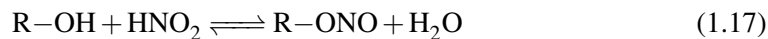
Equations 1.7 - 1.10 describe a possible branched radical chain mechanism, fed by the nitrous and nitric acids produced during the hydrolysis and alchohol oxidation reactions during the initiation stage. By contrast, the propagation reactions in the branched radical chain mechanism for thermolysis are poorly characterised (equation 1.2), defined only by the observable products. This is likely due to their rapid and varied nature, rendering it difficult to follow spectroscopically.

Aellig *et al.* presented an alternative scheme for the decomposition of benzyl nitrate ($R = PhCH_2$), involving more interaction with the solvent [7]:

Both the Camera/Chin and Aellig schemes above produce final end products observed in the decomposition of **NC!**. In particular, Aellig's scheme accounts for the production of N_2O, which forms a significant part of the decomposition eluent [8]. Whilst the schemes do not a propose an exhaustive description of the full spectrum of reactions that take place in the **NC!** matrix during its slow ageing, the early stage reactions of the key species responsible for decomposition are encapsulated.

It is widely agreed that first-stage decomposition follows a first-order process (or pseudo-first order, with respect to hydrolysis reactions). A number of studies observe catalytic rate of decay for the longer-term aging processes. Dauerman [9] observed that when **NC!** was treated with NO_2 gas before heating, the time required for sample ignition halved. He suggested that the NO_2 adsorbed onto the surface acted as a catalysing agent.

Neutral and alkaline hydrolysis reactions follow a pseudo-first order process, however

HNO$_3$ decomposition initiated

$$4\,HNO_3 \rightleftharpoons 4\,{}^{\bullet}NO_2 + 2\,H_2O + O_2 \tag{1.14}$$

$$2\,{}^{\bullet}NO_2 + H_2O \rightleftharpoons N_2O_4 + H_2O \tag{1.15}$$

$$N_2O_4 + H_2O \longrightarrow HNO_3 + HNO_2 \tag{1.16}$$

Propagation

$$R-OH + HNO_2 \rightleftharpoons R-ONO + H_2O \tag{1.17}$$

$$R-ONO \longrightarrow R{=}O + HNO \tag{1.18}$$

$${}^{\bullet}NO_2 + HNO \longrightarrow HNO_2 + {}^{\bullet}NO \tag{1.19}$$

$$2\,{}^{\bullet}NO + O_2 \longrightarrow 2\,{}^{\bullet}NO_2 \tag{1.20}$$

Termination

$$2\,HNO \longrightarrow HON{=}NOH \tag{1.21}$$

$$HON{=}NOH \longrightarrow N_2O + H_2O \tag{1.22}$$

it has been suggested that the presence of acid facilitates a catalytic rate of degradation after an initial incubation period. Multiple studies have addressed the decomposition reactions of nitrate esters following the initial scission of the nitrate group [10, 5, 11, 12, 1] In their work looking into the atmospheric reactions methyl nitrate methylperoxy nitrate Arenas (2007) suggested it was possible for the homolytic denitration reaction of methyl nitrate to share a common peroxy intermediate with the peroxide. This could account for some of the different/lower order NO_x generated (just ${}^{\bullet}NO$, tbh, or maybe perhaps how NO3 may get generated?).

In this section, secondary and extended reaction schemes for the low temperature ageing of **NC!** are explored. Decompostition pathways defined by Chin, Camera and Aellig *et al.* are probed to determine the reactions responsible for the experimentally observed degradation products. The reactions found to be energetically feasible from the proposed routes will be scrutinised to determine whether an autocatalytic pathway can be formed from the thermodynamically validated reaction schemes.

1.2   Methodology

The schemes proposed by Chin, Camera and Aellig *et al.* were used to construct possible degradation routes for **NC!** with the products of homolytic fission, elimination of HNO_2 and acid hydrolysis used as the starting point. Pathways were constructed based on propagation of the given reactions in a step-wise fashion; subsequent reactions were dependent on the

products generated in preceding steps. An abundance of water and oxygen were assumed present in the system, attributed to air exposure under the wetted storage conditions of **NC!**. Unsubsitutued alcohol moieties (R-OH) were also presumed available, due to incomplete nitration during the synthesis of **NC!** [13], and re-generation following denitration *via* hydrolysis. The schemes were modelled with both ethyl nitrate and the **NC!** monomer. Free energies of reaction (Δ G) were used to determine the feasibility of each reaction.

1.2.1 Computational details

All geometry optimisations were conducted in **G09!** (**G09!**), using the **wb97xd!** and **B3LYP!** functionals. Optimisations and thermochemistry calculations were performed to the level of 6-31+G(2df,p) with tight convergence criteria (table **??**). Calculations were performed in both vacuum and with **PCM!** (**PCM!**) to introduce implicit solvent effects. Chemical species were constructed using **GView!** (**GView!**) and for molecules of more than 3 atoms, the "Clean" function was used to re-order atoms to a preliminary starting geometry. Energies of optimised structures were checked against values listed on NIST Computational Chemistry Comparison and Benchmark Database [14] if analogous molecules to a similar level of theory were available.

1.3 Results and Discussion

Simplified schemes for the ageing reactions of **NC!** beginning from homolytic fission, elimination of HNO_2 or acid hydrolysis are illustrated in schemes 1.1 - 1.3.

When starting with the products of homolytic fission, a branched radical chain mechanism dominates. ˙NO_2 and HNO_2 were consumed and regenerated, supporting the theory that these may be species contributing to the observed autocatalytic rate of decomposition, following a first-order rate induction period [15, 16, 17]. For all schemes, R=O and N_2O were terminating species, which may go on to participate in wider reactions outside the scope of the proposed reactions. Table **??** shows the energies for the reactions in all schemes, for both ethyl nitrate and the **NC!** monomer.

Still to mention:

- Describe the other two schemes

- Describe the energies in the table

- Discuss why some of the values may be positive.

- Include enthalpies of reaction, zero point energies, and any experimental proxies I can find
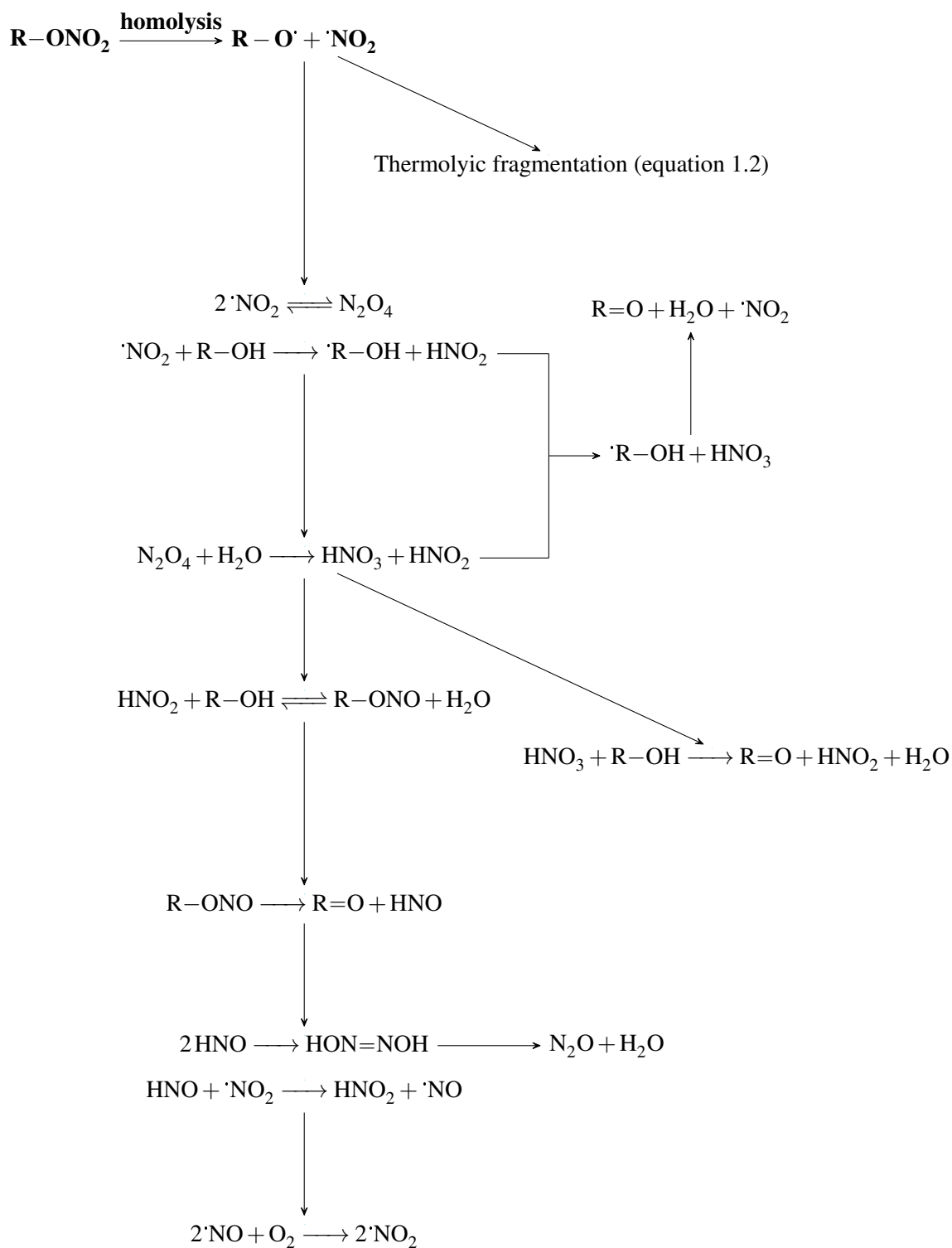
for the reaction enthalpies too.

NOTE: ZPE energy correction means that you REMOVE the ZPE, so that you only compare the actual energy available for the reaction. - ?

Table 1.1: Energies of nitrate ester decomposition reactions proposed by Camera [5], Chin [4] and Aellig [7]. R = CH_3CH_2 for ethyl nitrate, and R = $(H_3CO)_2C_6H_9O_3$ (bi-methoxy capped glucopyraonse monomer unit).

Reaction	ΔG_r /kcal mol^{-1}			
	wb97xd!	PCM	**B3LYP!**	PCM
$N_2O_4 + H_2O \longrightarrow HNO_3 + HNO_2$	2.25	1.85	5.13	4.18
$N_2O_4 \rightleftharpoons 2\,^{\cdot}NO_2$	0.12	1.46	−0.54	−0.16
Radical reactions				
$2\,^{\cdot}NO_2 \rightleftharpoons N_2O_4$	−0.12	−1.31	0.54	0.16
$^{\cdot}NO_2 + HNO \longrightarrow HNO_2 + \,^{\cdot}NO$	−28.22	−28.67	−27.33	−27.63
$2\,^{\cdot}NO + O_2 \longrightarrow 2\,^{\cdot}NO_2$	−20.77	−21.97	−21.16	−22.16
$2\,^{\cdot}NO + O_2 \longrightarrow 2\,^{\cdot}NO_2$	−59.89	−60.47	−60.47	−61.00
Acid reactions				
$HNO_3 + HNO_2 \rightleftharpoons N_2O_4 + H_2O$	−2.25	−1.85	−5.13	−4.18
$4\,HNO_3 \rightleftharpoons 4\,NO_2 + 2\,H_2O + O_2$	53.35	58.36	42.61	46.94
$2\,HNO \longrightarrow HON{=}NOH$	−38.97	−39.72	−36.63	−37.41
$HON{=}NOH \longrightarrow N_2O + H_2O$	−48.08	−48.18	−50.55	−50.75
Ionic reactions				
$NO_2{}^+ + 2\,H_2O \rightleftharpoons HNO_3 + H_3O^+$	−0.90	−1.34	1.77	2.46
Ethyl nitrate (R = CH_3CH_2)				
$R{-}ONO_2 + H_2O \longrightarrow R{-}OH + HNO_3$	4.56	5.24	4.00	4.86
$R{-}OH + HNO_3 \longrightarrow R{=}O + HNO_2 + H_2O$	−34.06	−38.43	−37.59	−41.77
$R{-}OH + \,^{\cdot}NO_2 \longrightarrow \,^{\cdot}R{-}OH + HNO_2$	16.38	13.92	15.89	13.70
$^{\cdot}R{-}OH + HNO_3 \longrightarrow R{=}O + H_2O + \,^{\cdot}NO_2$	−50.44	−52.35	−53.48	−55.47
$R{-}OH + HNO_2 \rightleftharpoons R{-}ONO + H_2O$	−3.21	−3.28	−2.64	−2.95
$R{-}ONO \longrightarrow R{=}O + HNO$	−1.50	−5.82	−4.37	−8.50
NC! monomer (R = $(H_3CO)_2C_6H_9O_3$)				
$R{-}ONO_2 + H_2O \longrightarrow R{-}OH + HNO_3$	0.68	5.63	0.61	−0.70
$R{-}OH + \,^{\cdot}NO_2 \longrightarrow \,^{\cdot}R{-}OH + HNO_2$	14.71	11.15	13.03	23.21
$^{\cdot}R{-}OH + HNO_3 \longrightarrow R{=}O + H_2O + \,^{\cdot}NO_2$	−51.44	−49.49	−54.75	−56.37
$R{-}OH + HNO_2 \rightleftharpoons R{-}ONO + H_2O$	−4.43	−7.30	−4.31	−0.18
$R{-}ONO \longrightarrow R{=}O + HNO$	−2.93	−1.71	−6.82	−11.21

Due to the availability of oxygen sites on the ethyl nitrate molecule, the optimal site for protonation was determined for inclusion in the reaction scheme for the first stage of hydrolysis. Table 1.2 shows the protonation energies for the three different oxygen sites on ethyl nitrate. Despite the upper terminal oxygen possessing the most thermodynami-

$$R-ONO_2 \xrightarrow{\text{homolysis}} R-O^{\cdot} + {}^{\cdot}NO_2$$

Thermolyic fragmentation (equation 1.2)

$$2\,{}^{\cdot}NO_2 \rightleftharpoons N_2O_4$$

$$R{=}O + H_2O + {}^{\cdot}NO_2$$

$${}^{\cdot}NO_2 + R-OH \longrightarrow {}^{\cdot}R-OH + HNO_2$$

$${}^{\cdot}R-OH + HNO_3$$

$$N_2O_4 + H_2O \longrightarrow HNO_3 + HNO_2$$

$$HNO_2 + R-OH \rightleftharpoons R-ONO + H_2O$$

$$HNO_3 + R-OH \longrightarrow R{=}O + HNO_2 + H_2O$$

$$R-ONO \longrightarrow R{=}O + HNO$$

$$2\,HNO \longrightarrow HON{=}NOH \longrightarrow N_2O + H_2O$$

$$HNO + {}^{\cdot}NO_2 \longrightarrow HNO_2 + {}^{\cdot}NO$$

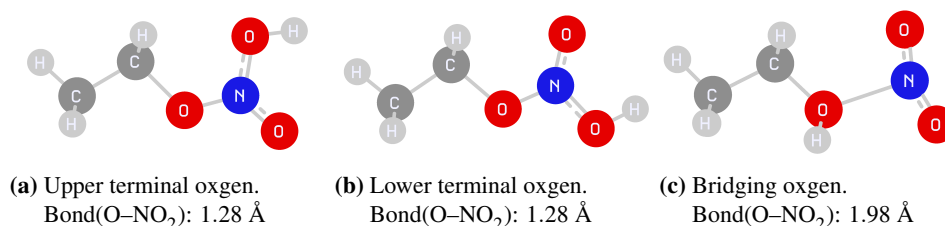$$2\,{}^{\cdot}NO + O_2 \longrightarrow 2\,{}^{\cdot}NO_2$$

Scheme 1.1: Proposed degradation pathway starting from the homolytic fission of the nitrate ester, derived from the schemes presented by Camera [5] and Aellig[7].

Table 1.2: Free energies of protonation for each oxygen site on ethyl nitrate.

Protonated site		ΔG_r /kCal mol^{-1}			
		wb97xd!	PCM	**B3LYP!**	PCM
Terminal (upper)	$CH_3CH_3ONO_2H^+$	-12.28	8.82	-13.78	5.63
Terminal (lower)	$CH_3CH_3ONO_2H^+$	-9.48	9.46	-11.13	5.65
Bridging	$CH_3CH_3O(H^+)NO_2$	-9.32	9.06	-15.31	6.67

(a) Upper terminal oxgen.
Bond(O–NO$_2$): 1.28 Å

(b) Lower terminal oxgen.
Bond(O–NO$_2$): 1.28 Å

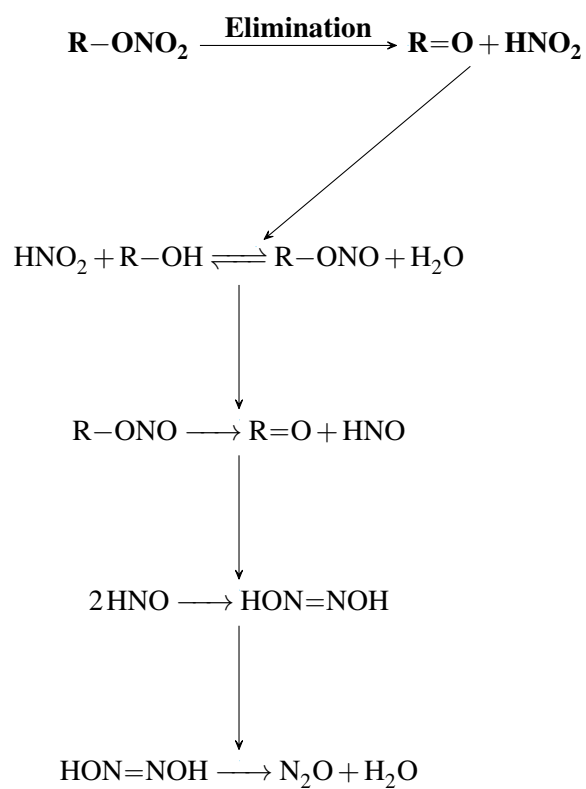**(c)** Bridging oxgen.
Bond(O–NO$_2$): 1.98 Å

Figure 1.4: Optimised geometries of the possible protonation sites on ethyl nitrate.

cally favourable energy of protonation, inspection of the reaction geometries shows that the bridging structure most resembles that expected for the liberation of the NO_2^+ group at the next step. Though appearing less thermodynamically favourable when compared to proto-nation at the terminal upper oxygen site, the higher energy of reaction likely arises from the instability of the protonated complex. The elongation of the O–NO$_2$ bond allows to stabili-sation of the proton at the bridging site, such that the departure of NO_2^+ is easily facilitated. Subsequent calculation involving the energy of the protonated ethyl nitrate will employ the values associated with the protonated bridging site.
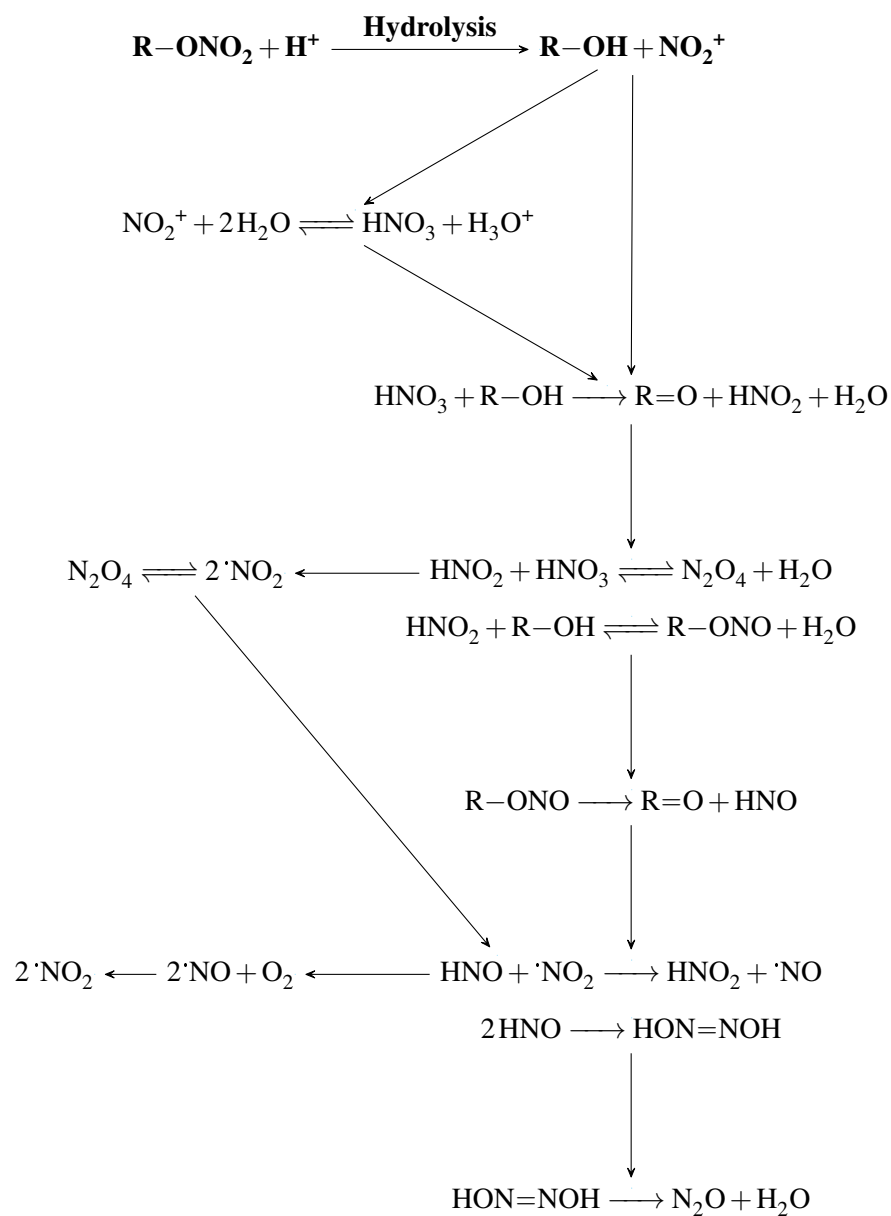
For the decomposition of HNO_3 to .NO_2, $2H_2O$ and O_2, Aellig prescribes the use of an amberlyst catalyst (amberlyst-15).

1.4   Summary

Map of the possible reactions, linking to

$$\text{R--ONO}_2 \xrightarrow{\textbf{Elimination}} \text{R=O} + \text{HNO}_2$$

$$\text{HNO}_2 + \text{R--OH} \rightleftharpoons \text{R--ONO} + \text{H}_2\text{O}$$

$$\text{R--ONO} \longrightarrow \text{R=O} + \text{HNO}$$

$$2\,\text{HNO} \longrightarrow \text{HON=NOH}$$

$$\text{HON=NOH} \longrightarrow \text{N}_2\text{O} + \text{H}_2\text{O}$$

Scheme 1.2: Proposed degradation pathway starting from the elimination of HNO_2 from a nitrate ester, derived from the schemes presented by Camera [5] and Aellig[7].

$$\mathbf{R-ONO_2 + H^+} \xrightarrow{\textbf{Hydrolysis}} \mathbf{R-OH + NO_2^+}$$

$$NO_2^+ + 2H_2O \rightleftharpoons HNO_3 + H_3O^+$$

$$HNO_3 + R-OH \longrightarrow R{=}O + HNO_2 + H_2O$$

$$N_2O_4 \rightleftharpoons 2\,{}^{\bullet}NO_2 \longleftarrow HNO_2 + HNO_3 \rightleftharpoons N_2O_4 + H_2O$$

$$HNO_2 + R-OH \rightleftharpoons R-ONO + H_2O$$

$$R-ONO \longrightarrow R{=}O + HNO$$

$$2\,{}^{\bullet}NO_2 \longleftarrow 2\,{}^{\bullet}NO + O_2 \longleftarrow HNO + {}^{\bullet}NO_2 \longrightarrow HNO_2 + {}^{\bullet}NO$$

$$2\,HNO \longrightarrow HON{=}NOH$$

$$HON{=}NOH \longrightarrow N_2O + H_2O$$

Scheme 1.3: Proposed degradation pathway starting from the acid hydrolysis of a nitrate ester, derived from the schemes presented by Camera [5] and Aellig[7].

Bibliography

[1] K. S. Hu, A. I. Darer, and M. J. Elrod. Thermodynamics and kinetics of the hydrolysis of atmospherically relevant organonitrates and organosulfates. *Atmospheric Chemistry and Physics*, 11(16):8307–8320, aug 2011.

[2] M. Moniruzzaman and J.M. Bellerby. Use of UV-visible spectroscopy to monitor nitrocellulose degradation in thin films. *Polymer Degradation and Stability*, 93(6):1067–1072, jun 2008.

[3] Mohammed Moniruzzaman, John M. Bellerby, and Manfred A. Bohn. Activation energies for the decomposition of nitrate ester groups at the anhydroglucopyranose ring positions C2, C3 and C6 of nitrocellulose using the nitration of a dye as probe. *Polymer Degradation and Stability*, 102:49–58, apr 2014.

[4] Anton Chin, Daniel S. Ellison, Sara K. Poehlein, and Myong K. Ahn. Investigation of the Decomposition Mechanism and Thermal Stability of Nitrocellulose/Nitroglycerine Based Propellants by Electron Spin Resonance. *Propellants, Explosives, Pyrotechnics*, 32(2):117–126, apr 2007.

[5] E. Camera, G. Modena, and B. Zotti. On the Behaviour of Nitrate Esters in Acid Solution. II. Hydrolysis and oxidation of nitroglycol and nitroglycerin. *Propellants, Explosives, Pyrotechnics*, 7(3):66–69, jun 1982.

[6] Fotis Rigas, Ioannis Sebos, and Danae Doulia. Safety Charts Simulation of Nitroglycerine/Nitroglycol Spent Acids via Chemical Reaction Kinetics. *Industrial and Engineering Chemistry Research*, 36(12):5068–5073, 1997.

[7] Christof Aellig, Christophe Girard, and Ive Hermans. Aerobe Alkoholoxidation mithilfe von HNO3. *Angewandte Chemie*, 123(51):12563–12568, dec 2011.

[8] S. J. Buelow, D. Allen, G. K. Anderson, F. L. Archuleta, and J. H. Atencio. Destruction of Energetic Materials in Supercritical Water. Technical report, AIR FORCE RESEARCH LABORATORY, 2002.

[9] L. Dauerman and Y. A. Tajima. Thermal decomposition and combustion of nitrocellulose. *AIAA Journal*, 6(8):1468–1473, aug 1968.

[10] John W. Baker and D. M. Easty. Hydrolytic decomposition of esters of nitric acid. Part I. General experimental techniques. Alkaline hydrolysis and neutral solvolysis of methyl, ethyl, isopropyl, and tert.-butyl nitrates in aqueous alcohol. *Journal of the Chemical Society (Resumed)*, 1952(0):1193–1207, 1952.

[11] E. Camera, G. Modena, and B. Zotti. On the behaviour of nitrate esters in acid solution. III. Oxidation of ethanol by nitric acid in sulphuric acid. *Propellants, Explosives, Pyrotechnics*, 8(3):70–73, jun 1983.

[12] V. G. Matveev and G. M. Nazin. Stepwise Degradation of Polyfunctional Compounds. *Kinetics and Catalysis*, 44(6):735–739, nov 2003.

[13] Frank E. Wolf. Alkaline Hydrolyis Conversion of Nitrocellulose Fines. Technical Report October, Badger Army Ammunition Plant, oct 1997.

[14] Russell D. Johnson III. NIST Computational Chemistry Comparison and Benchmark Database NIST Standard Reference Database Number 101, 2018.

[15] I. Rodger and J. D. Mcirvine. The decomposition of spent PETN nitration acids. *The Canadian Journal of Chemical Engineering*, 41(2):87–90, apr 1963.

[16] Torbjórn Lindblom. Reactions in stabilizer and between stabilizer and nitrocellulose in propellants. *Propellants, Explosives, Pyrotechnics*, 27(4):197–208, sep 2002.

[17] Hermann N. Volltrauer and Arthur Fontijn. Low-temperature pyrolysis studies by chemiluminescence techniques real-time nitrocellulose and PBX 9404 decomposition. *Combustion and Flame*, 41:313–324, jan 1981.